MAP1B and Clathrin Are Novel Interacting Partners of the Giant Cyto-linker Dystonin

ARTICLE *in* JOURNAL OF PROTEOME RESEARCH · SEPTEMBER 2011

Impact Factor: 4.25 · DOI: 10.1021/pr200564g · Source: PubMed

3 AUTHORS, INCLUDING:

Kevin G Young
Ottawa Hospital Research Institute
17 PUBLICATIONS **387** CITATIONS
SEE PROFILE

Rashmi Kothary
Ottawa Hospital Research Institute
149 PUBLICATIONS **4,543** CITATIONS
SEE PROFILE

Journal of proteome research

ARTICLE

pubs.acs.org/jpr

MAP1B and Clathrin Are Novel Interacting Partners of the Giant Cyto-linker Dystonin

Kunal Bhanot,[†] Kevin G. Young,[†,‡] and Rashmi Kothary*[,†,§]

[†]Regenerative Medicine Program, Ottawa Hospital Research Institute, 501 Smyth Road, Ottawa, Ontario, Canada, K1H 8L6

[§]The Department of Cellular and Molecular Medicine and The Department of Medicine, University of Ottawa, Ottawa, Ontario, Canada

Supporting Information

ABSTRACT: Dystonin is a large multidomain cytoskeletal-associated protein that plays an essential role in the nervous system. Loss of dystonin results in neuromuscular dysfunction and early death in a mouse mutant called *dystonia musculorum*. Conserved among related proteins, the plakin domain is a defining feature of all major dystonin isoforms, yet its interactions have not been explored in detail. The purpose of the present study was to identify novel interacting partners of the plakin domain of the neuronal isoform of dystonin (dystonin-a). Newly identified interacting proteins discovered through a pull-down assay were validated using coimmunoprecipitation, coimmunofluorescence, and proximity ligation assays. Microtubule associated protein 1B (MAP1B), a microtubule stabilizing protein, and clathrin heavy chain, the major component of the clathrin triskelion, were identified as interaction partners for dystonin-a. Increased levels of phosphorylated MAP1B suggest a misregulation of MAP1B and a potentially novel component of the *dt* pathology. This work will further facilitate our understanding of how cytoskeletal proteins can affect and regulate neurodegenerative disorders.

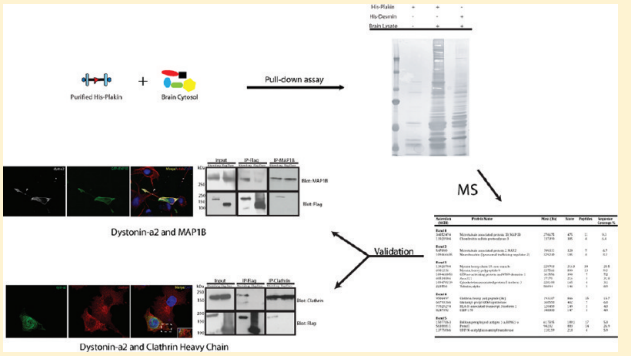

KEYWORDS: dystonin, BPAG1, dystonia musculorum, neurodegeneration

INTRODUCTION

Cytoskeletal plasticity arises through various arrangements and assortments of the main cytoskeletal structures, namely actin microfilaments, intermediate filaments and microtubules.[1,2a] These arrangements are made possible by cytoskeletal cross-linking proteins. The plakin family of proteins is a major group of cyto-linkers. This family comprises several structurally related proteins with various cytoskeletal-binding domains. Members include desmoplakin, microtubule actin cross-linking factor 1 (MACF1)/Acf7, envoplakin, periplakin and dystonin.[2b,2c] The dysfunction of members of this family are implicated in several skin, muscle, and neuronal disorders such as paraneoplastic pemphigus, striate palmoplantar keratoderma, bullous pemphigoid, and epidermolysis bullosa simplex with muscular dystrophy.[1,3]

Loss of dystonin function results in a severe neuromuscular phenotype in the mouse mutant *dystonia musculorum* (*dt*).[4−7] The gradual loss of nerve fibres in the peripheral and central regions of the sensory pathways with focal swellings along the affected fibers is characteristic of this condition.[7] Degeneration occurs within the sensory root of the spinal cord ganglia and the cranial nerves of *dt* mice and involves neurofilament and microtubule aggregation.[7−10] Abnormalities in the neuronal cell bodies include nuclear eccentricity and the dispersion of the rough endoplasmic reticulum from around the nucleus.[11] More recently, motor neuron defects have been described that likely also contribute to the *dt* pathology.[12]

Alternative splicing giving rise to multiple isoforms is a common feature for the plakin protein family.[1] The Dst gene gives rise to several complex transcripts producing isoforms found in skin (dystonin-e), nervous system (dystonin-a) and muscle (dystonin-b). Alternative splicing at the N-terminal end just upstream from an actin-binding domain (ABD) results in the generation of several variants for the neuronal and muscle isoforms.[13,14] These isoforms are referred to as dystonin-a1, dystonin-a2, and dystonin-a3 for neuronal dystonin and dystonin-b1, dystonin-b2, and dystonin-b3 for muscle dystonin.[14] Isoforms 2 and 3 possess a transmembrane domain and a putative myristoylation motif, respectively, and evidence suggests that these proteins are membrane-associated.[15,16] The one common feature of all isoforms is the presence of the family defining plakin domain, downstream of the ABD in the dystonin-a and dystonin-b proteins. The role of this domain is, however, not well-defined.

Nesprin 3α, actin, and microtubules are just a few of the already identified interactors of dystonin.[11,15,17−19] However, based on its modular structure, it is likely that dystonin is involved in many other interactions. Previous characterization of the nonepithelial dystonin proteins has focused on the alternate N-terminal ends and the C-terminal microtubule-binding domain. Interactions of the plakin domain are limited to a demonstration of its ability to

Received: June 11, 2011
Published: September 21, 2011

bind BP180 in epithelial cells[20] and a likely involvement in binding to ERBIN.[21] Jefferson et al. proposed that the plakin domain of dystonin is composed of two pairs of spectrin repeats separated by a Src-homology 3 (SH3) domain.[21b] The SH3 domain is a conserved region that is generally found in proteins that mediate interactions and complex formations with other proteins by binding to proline-rich peptide sequences.[22−24] This region is central to the interaction ability of other spectrin superfamily members such as α1-spectrin, which is known to dimerize with β-spectrin.[25] Therefore, the SH3 domain of dystonin may be an important interacting region.

The purpose of the present study was to identify novel interacting partners of dystonin in an effort to elucidate the functions of this complex protein. As the loss of a specific isoform, dystonin-a2, is believed to be causative for the *dt* phenotype,[3] our analyses focused on this neuronal isoform of dystonin. As the large size and multidomain structure of dystonin make it difficult to perform interaction studies on the entire protein, we directed our efforts specifically to the plakin domain. Through pull-down interaction analyses we have identified MAP1B as an interaction partner of dystonin-a2. The known associations of MAP1B with components of the cytoskeleton further support dystonin's role as a cytoskeletal linker protein. Additionally, new possibilities for the *dt* pathology are proposed through the misregulation of phosphorylated MAP1B. Further, the identification and validation of an interaction with clathrin heavy chain, the major component of the clathrin triskelion involved in intracellular transport and endocytosis, suggests new roles for the dystonin protein.

METHODS

Recombinant Protein Plasmids

Bacterial expression: A his-tagged plakin (his-plakin) plasmid was generated using the pET30c(+) vector (Novagen) and encoded the plakin domain of dystonin-a/b (base pair 1512−base pair 4644 GenBank Accession NM133833.2) flanked by his-tags at both the N and C-terminal ends (supplemental, Figure S1). The T7 promoter drove expression of the his-tagged plakin coding region. His-tagged desmin (his-desmin) was generated by incorporating the desmin coding sequence (base pair 66−base pair 787 GenBank Accession NM010043.1) into the pET30c(+) vector, which has linkers coding for his-tags at both the N and C-terminal ends (Supporting Information, Figure S1).

Mammalian expression: A flag-tagged fusion plasmid expressing part of the N-terminal domain of dystonin in addition to the entire plakin domain (Ntermlong) was used to perform coimmunoprecipitation reactions as part of the interaction validation experiments.[17] Flag-tagged death associated protein (Daxx) was used a negative control for the coimmunoprecipitation validation experiments. For coimmunofluorescence analysis and proximity ligation assay, a C-terminus myc-tagged dystonin isoform-a2 (dyst-a2) mammalian expression construct[11] was used in addition to an N-terminal-green fluorescence protein-tagged MAP1B (GFP-MAP1B).

Pull-down Assays

The purified fusion proteins (Supporting Information, Figure S2) bound to the purification beads (Ni-NTA, Novagen) were incubated with the cytosolic fraction of whole brain rat pup lysate (600 μg) for 4 h at 4 °C with gentle agitation. The purification beads bound to the fusion protein along with any potential plakin binding partners were centrifuged at 4 °C. For the his-plakin construct, the bead-plakin-partner complex was washed multiple times with 100 mM imidazole solution followed by centrifugation. The his-plakin fusion protein along with any potential binding partners was eluted off of the purification beads with 500 mM imidazole. The eluate was analyzed by SDS-PAGE. The same procedures were performed in parallel for the his-desmin negative control.

Cell Culture

Cos-1 monkey kidney and F11 mouse neuroblastoma rat dorsal root ganglia (DRG) hybrid cell lines were cultured in DMEM (Dulbecco's modified eagle media) (Wisent) with 10% fetal bovine serum (FBS) (Sigma). Cells were cultured in 10 cm plates (Corning) for protein extraction. For immunofluorescence, cells were cultured on glass coverslips in 12-well plates (Corning). Cells were transfected using Lipofectamine 2000 (Invitrogen) according to the manufacturer's protocol for each cell type. Transfected cells were cultured for 24 h prior to performing any analyses. When necessary, F11 cells were differentiated using 0.5 mM dibutyryl cyclic adenosine monophosphate (db-cAMP, Sigma) in DMEM post-transfection.

Protein extraction

Adherent cell culture. Cell culture plates were washed with PBS and incubated with lysis buffer containing protease and phosphatase inhibitors (50 mM Tris-HCl pH 7.4, 150 mM NaCl, 2 mM EDTA, 1% NP-40, 1 μg/mL leupeptin, 1 μg/mL aprotinin, 5 μg/mL PMSF, 1 μg/mL pepstatin) on ice for 5 min. Lysate containing tubes were gently agitated for 30 min at 4 °C. The tubes were then centrifuged and the soluble and insoluble fractions were either used immediately or stored at −80 °C for further analysis.

Whole tissue lysate. Wild-type and *dt* animals were sacrificed by cervical dislocation. Protein extracts were obtained from dissected DRGs by homogenizing in chilled RIPA buffer containing a cocktail of protease and phosphatase inhibitors (50 mM Tris-HCl pH 7.4, 150 mM NaCl, 2 mM EDTA, 1% NP-40, 0.1% SDS 1 μg/mL leupeptin, 1 μg/mL aprotinin, 5 μg/mL PMSF, 1 μg/mL pepstatin). The samples were then centrifuged for 15 min at 4 °C and the supernatant was either stored at −80 °C or used immediately for further analysis.

Mass Spectrometry

Mass spectrometry was performed at the Ottawa Institute of Systems Biology. In-gel digestion was performed as described previously.[26,27] Trypsin (Promega) digestions were performed for 16 h. Extracted peptides were hydrated in 20 mL of 5% formic acid and analyzed by LC−MS/MS. An Agilent (Agilent Technologies) 1100 series HPLC system was used to load peptides onto a precolumn packed with 5 μm YMC ODS-A C_{18} beads (Waters). The eluate was then applied to a second column packed with the same beads using a 5−80% gradient of acetonitrile with 0.1% formic acid for 1 h. LTQ linear ion-trap mass spectrometer (Thermo-Electron) was electrosprayed with the LC effluent. The four most intense peaks from each MS spectrum generated were used to provide the MS/MS spectra. Tolerances were set at 6.2 and 0.8 Da for the peptide and MS/MS respectively. MS/MS data were then analyzed and matched to rat protein sequences in the NCBI database (nrdb) using the MASCOT database search engine version: 2.2.04 (MatrixScience). An ion score cutoff of 40 ensured a false positive rate of less than 5%. This score was based on a previous large scale proteomic analysis that demonstrated

tryptic peptides with +2 and +3 charges could be identified with approximately 99% precision using cutoff scores of 30 and 26.[28]

Coimmunoprecipitation

Protein isolated from transfected adherent cell cultures was used in coimmunoprecipitation analysis. After overnight preclearing, soluble lysates (500 μg) containing flag-tagged constructs were incubated with Sepharose protein G beads (50 μL bed volume, GE healthcare) or Dynal protein G magnetic beads (50 μL bed volume, Invitrogen) along with 5 μg of the appropriate antibody overnight at 4 °C on a rocking platform. The tubes were either centrifuged or placed on a magnetic rack according to the manufacturer's specification. Washes were performed and the flag-tagged proteins were eluted off of the beads using 0.1 M glycine pH 3.0. Protein loading buffer was added to the eluted samples (60 mM Tris pH 6.8, 2% SDS, 10% glycerol), which were then boiled for 5 min. PAGE was performed on the eluates and the protein was then transferred to a PVDF membrane, which was probed for the coimmunoprecipitated partners.

Immunofluorescence

Cells (Cos-1 and F11) were grown on coverslips in appropriate cell culture media. Cells were fixed with 4% PFA (pH 7.4) for 10 min followed by PBS washes. Samples were then incubated at room temperature with blocking solution (PBS, 0.4% Triton X-100, 10% goat serum). Appropriate primary antibodies were diluted in the antibody solution (PBS, 0.4% Triton X-100, 0.5% bovine serum albumin) overnight at 4 °C. The samples were then washed with PBS. Appropriate secondary antibodies and DAPI nuclear stain (1 ng/mL) were diluted in the same solution used for the primary antibody and incubated with the samples for 1 h at room temperature. PBS washes were performed and the cells grown on coverslips and stained were then mounted onto microscope slides (Fisher premium frosted). Micrographs were obtained using Zeiss LSM 510 and LSM 700 confocal microscopes. Image analysis was done using Abode Photoshop CS4 and ImageJ software.

Proximity Ligation Assay

Proximity ligation assay (PLA) was performed as previously described.[27] Briefly, cells were plated on coverslips in a 12-well plate at a density of 40 000 cells per well. For the MAP1B-dystonin-a2 PLA, F11 cells were transfected with dyst-a2 and GFP-MAP1B and differentiated for 48 h. Cells were washed with PBS and fixed with 4% PFA (pH 7.4). After incubation with blocking solution (PBS, 0.4% Triton X-100, 10% goat serum) appropriate primary antibodies diluted in the antibody solution (PBS, 0.4% Triton X-100, 0.5% bovine serum albumin) were added and left overnight at 4 °C. The remaining steps of the protocol were performed at 37 °C in a humidity chamber using the reagents provided in the Duolink I PLA kit (Olink Bioscience). PLA probes (mouse-plus; rabbit-minus) were diluted 1:5 in antibody solution and left on the coverslips for 90 min. The probe solution was gently tapped off the coverslips, which were then washed with TBST (50 mM Tris, 150 mM NaCl, 0.05% Tween 20, PH 7.4). The hybridization stock solution diluted 1:5 in high purity water was then applied to the coverslips for 15 min. The hybridization solution was removed and the coverslips washed with TBST. The ligation solution, containing the ligation stock diluted 1:5 in high purity water along with ligase diluted 1:40, was added to the coverslips for 15 min. After tapping off the ligation solution and washing the coverslips with TBST, the amplification solution, containing amplification stock diluted 1:5 in high purity water in addition to polymerase diluted at 1:80, was applied to the coverslips for 90 min. Following removal of the amplification solution and subsequent TBST washes, the detection solution, containing detection stock diluted 1:5 in high purity water, was added to the coverslips for 30 min. In addition to being incubated in a 37 °C humidity chamber, the samples were now shielded from light. While continuing to shield from light, a series of SSC buffer (150 mM NaCl, 15 mM sodium citrate, pH 7.0) washes were performed. Secondary fluorescent antibodies (1:500, Invitrogen) along with DAPI nuclear stain was diluted in antibody solution and applied to the coverslips for 30 min. Several TBST washes were performed and the coverslips were then washed with 70% ethanol and allowed to dry in the dark. Once dried, the coverslips were mounted on slides and ready for imaging.

Mice

A mutation in the *Dst* locus of the congenic strain B10.PL(73N)/Sn gave rise to dt^{27J} mice which were originally identified by The Jackson Laboratory (Bar Harbor). The mice were housed in the vivarium facility of the University of Ottawa. The Animal Care Committee of the University of Ottawa approved experimental protocols on the mice. Care and use of experimental mice followed the guidelines of the Canadian Council on Animal Care. Postnatal day 15 animals were anaesthetized with ketamine/rompun (0.1 mg/g, 0.01 mg/g) delivered by intraperitoneal injection before excising the tissues.

Antibodies

For the immunoprecipitation reactions, 5 μg of the following antibodies were used: Flag (M2-Sigma, mouse), MAP1B (AA6 Sigma, mouse), Clathrin heavy chain (Abcam, rabbit). Immunoblotting was performed with the following antibodies: Flag (1:15 000, M2-Sigma, mouse), MAP1B (1:5000, AA6-Sigma, mouse), clathrin heavy chain (1:500, Cell Signaling, rabbit), SMI-31 (1:1000, Abcam, mouse), tubulin (1:1000, E7-supernatant, mouse). Immunofluorescence was performed using the following antibodies in addition to DAPI nuclear stain: C-Myc (1:750, 9E10-Santa Cruz, mouse), Clathrin heavy chain (1:500, Abcam, rabbit). PLA was performed using the following antibodies: C-Myc (1:750, 9E10-Santa Cruz, mouse), GFP (1:500, Invitrogen, rabbit), Clathrin heavy chain (1:500, Abcam, rabbit). Appropriate Alexa Fluor secondary antibodies were used at a concentration of 1:500 where applicable.

RESULTS

Plakin Binding Partners Identified through a Pull-down Analysis

Purified soluble his-plakin protein was incubated with a cytosolic fraction of whole brain lysate from rat pups. Figure 1A depicts a schematic representation of the fusion plasmids used for the pull-down assay as well as the interaction analysis. Full-length myc-tagged dystonin-a2 (630 kDa, dyst-a2) provides the context for the regions possessed by the smaller fusion plasmids used in the interaction assays. The potential interacting partners of his-plakin were excised from a silver stained acrylamide gel and subjected to tryptic digestion (Figure 1B). His-tagged desmin (his-desmin), an intermediate filament protein, was produced and purified in the same manner as the his-plakin fusion protein and used as a negative control (Figure 1B). Bands were only excised from the his-plakin + brain lysate lane if the corresponding bands were not present in either the his-plakin only lane or in the his-desmin + brain cytosol lane. Identification of potential partners unique to the his-plakin pull-down was performed using an LTQ linear ion trap mass

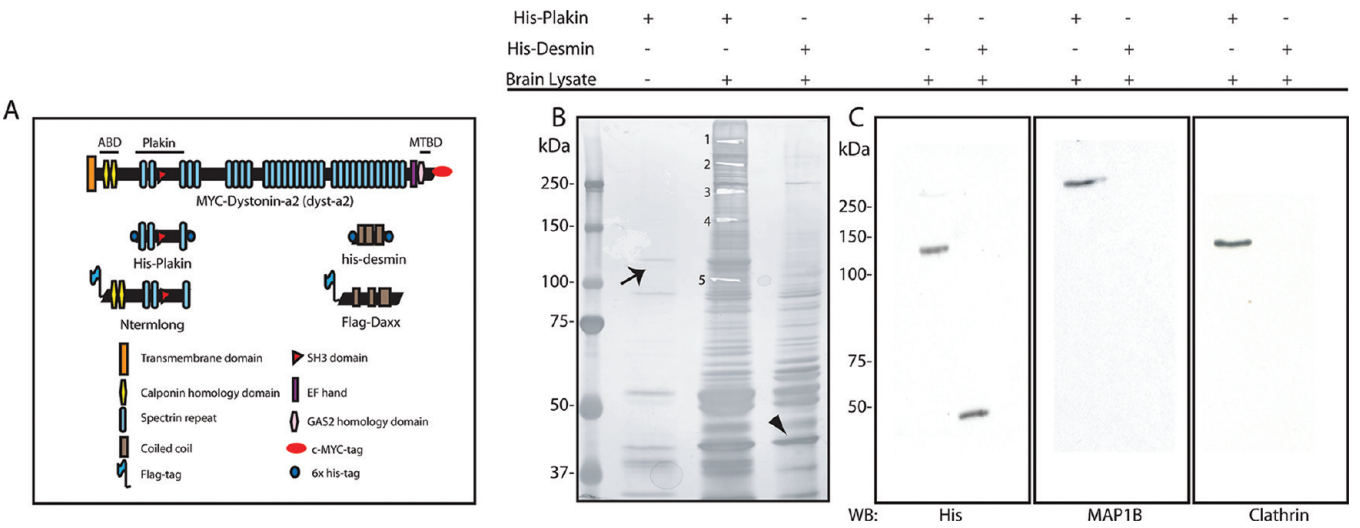

Figure 1. Pull-down of several novel his-plakin interactors. Purified his-plakin and his-desmin proteins were incubated with the cytosolic fraction of rat pup whole-brain lysate (brain-cytosol). PAGE was performed on the eluates from the pull-down experiments followed by silver staining to visualize the proteins. (A) Schematic representations of the fusion plasmids used in the pull-down in interaction validation experiments. (B) His-plakin fusion pull-down using the ~128 kDa his-plakin fusion protein. Lane 1 depicts the successful purification of the his-plakin protein (arrow). After the purification of the fusion proteins and just prior to their elution from the his-bind resin (Ni-NTA, Novagen), they were incubated with the cytosolic fraction of rat pup whole-brain lysate. Several unique bands were observed in the his-plakin with brain-cytosol lane when the gel was silver stained. Lanes 2 and 3 illustrate the bands remaining in the his-plakin with brain-cytosol and his-desmin (arrowhead) with brain-cytosol (negative control) eluates respectively, after the stringent wash protocol was performed. Bands present in lane 2, but not present in lanes 1 and 3, were excised and prepared for mass spectrometry analysis. Western blots were then performed on eluates used for the pull-down analysis. (C) Anti-his immunoblot detected expression of his-plakin (128 kDa) and his-desmin (68 kDa) in his-plakin with brain cytosol and his-desmin with brain cytosol lanes respectively. MAP1B and clathrin were detected only in the his-plakin with brain cytosol lane, indicating specificity in the pull-down analysis.

spectrometer. Several novel binding partners identified are listed in Table 1. Of the plakin domain partners identified, known associations with cytoskeletal elements and previous evidence of a role in cellular transport led us to perform validation experiments on MAP1B and clathrin heavy chain respectively.

Validation of Dystonin Plakin Domain Binding Partners

Immunoblots probing for MAP1B and clathrin heavy chain were performed on lysate from the pull-down analysis that was used for the mass spectrometry. MAP1B and clathrin heavy chain were observed to be present only with the his-plakin pull-down and not with the his-desmin pull-down (Figure 1C). Further validation experiments aimed at establishing the interaction legitimacy were performed on MAP1B and clathrin heavy chain.

Dystonin Colocalizes with MAP1B

F11 cells, which are a DRG-like hybrid immortalized cell line derived from rat DRG and mouse neuroblastoma, were transiently cotransfected with dyst-a2 and GFP-MAP1B, and subsequently differentiated (Figure 2A–D). Dyst-a2 was detected in 12% of the total cells observed, while GFP-MAP1B had a transfection efficiency of over 51% (~40 000 cells per well in a 12-well plate). Perinuclear colocalization of the dyst-a2 signal with GFP-MAP1B was observed in cotransfected cells (Figure 2). As MAP1B associates with microtubules, the overlapping pattern of dyst-a2 with MAP1B was observed to be along the microtubule network throughout the cell body (Figure 2A–D). This pattern of perinuclear and cytoplasmic localization was representative of 39% of the transfected cells.

MAP1B Association with Dystonin-a2 as Demonstrated through Proximity Ligation Assay

A PLA was also used to determine the veracity of the interaction between dystonin-a2 and MAP1B. A signal was detected in cells expressing both dyst-a2 and GFP-MAP1B in F11 cells (Figure 2E–G). The assay is supported by the lack of observable PLA signal in cells expressing only GFP-MAP1B (Figure 2G). A positive PLA control was also performed on Cos-1 cells transiently cotransfected with myc-tagged dystonin-N2 and GFP-nesprin3α (Supporting Information, Figure S3). The positive PLA signal supports evidence of this established interaction. The lack of signal from the PLA between dystonin-N2 and GFP- nesprin3ß further supports the specificity of this interaction assay.

Reciprocal Coimmunoprecipitation of MAP1B and the Dystonin Plakin Domain

Coimmunoprecipitation experiments using a dystonin N-terminus fusion protein (Ntermlong, ~170 kDa) and MAP1B were conducted in transiently transfected cells. As fusion proteins expressing only the plakin domain localize within the nucleus,[16] the use of a construct featuring the plakin domain along with other N-terminal dystonin components ensured localization of the constructs would be cytosolic. Flag-tagged death associated protein (Daxx, ~115 kDa) fusion construct was used as a negative control for the coimmunoprecipitation experiments to ensure that coimmunoprecipitation was not a result of nonspecific binding to the flag epitope. Endogenous MAP1B only reciprocally coimmunoprecipitated with transiently transfected Ntermlong and not with Daxx from differentiated F11 cells. This indicates that coimmunoprecipitation of MAP1B with the dystonin plakin domain fusion protein was not a result of nonspecific or background interactions (Figure 2H).

An immunoblot for the flag epitopes of the Ntermlong and Daxx constructs showed the presence of the fusion proteins in lysates from the transiently transfected and differentiated F11

dx.doi.org/10.1021/pr200564g |J. Proteome Res. 2011, 10, 5118–5127

Table 1. Plakin Domain Novel Binding Partners[a]

accession (NCBI)	protein name	mass (Da)	score	peptides	sequence coverage %
	Band 1				
34852474	Microtubule associated protein 1B, MAP1B	270 675	475	11	9.3
13928904	Chondroitin sulfate proteoglycan 3	137 399	305	4	6.4
	Band 2				
547890	Microtubule associated protein 2, MAP2	199 331	320	7	6.7
109466685	Neurobeachin (Lysosomal trafficking regulator 2)	329 240	185	4	3.2
	Band 3				
13928704	Myosin heavy chain 10, nonmuscle	229 793	2163	30	23.5
6981236	Myosin, heavy polypeptide 9	227 566	899	13	9.2
109468053	GTPase activation protein and VPS9 domains 1	161 556	390	7	7.2
68534846	Ascc311	17 175	216	3	31.8
109470239	Cytoskeleton associated protein 5 isoform 3	228 108	165	4	3.1
223556	Tubulin, alpha	50 894	146	3	8.9
	Band 4				
9506497	Clathrin, heavy polypeptide (Hc)	193 187	866	15	15.7
66793366	Glutamyl-prolyl-tRNA synthetase	168 558	462	7	6.8
77020274	HLA-B-associated transcript 3 isoform 1	120 450	149	3	4.3
8247352	CLIP-170	148 800	147	3	4.9
	Band 5				
15077863	Bullous pemphigoid antigen 1-a, BPAG1-a	617 595	1001	17	5.3
56388811	Psmd1	94 232	883	14	26.9
13775066	UDP-*N*-acetylglucosaminyltransferase	118 159	218	4	5.9

[a] Gel-excised protein band identification of targets through pull-down analysis of his-plakin with rat pup brain lysate through mass spectrometry. An ion score cut-off of 40 was selected to ensure a confidence level of above 95% in the targets identified. Accession refers to the National Centre for Biotechnology Information (NCBI) database. Score refers to the values indicated by the MASCOT search engine. Peptides used for protein identification either meet or exceed the minimum ion score cut-off set for an above 95% confidence level with repeat sequences excluded. Sequence coverage denotes the percentage of the total amino acid sequence spanned by the peptides detected.

cells, verifying expression and successful binding to the Sepharose protein G beads used for the immunoprecipitation reaction (Figure 2H). This lysate was also probed for the expression of endogenous MAP1B. A band at ~300 kDa indicates the expression of MAP1B in the input lysate (Figure 2H). The results from this coimmunoprecipitation analysis indicate that the plakin domain of dystonin possesses the capability of interacting with MAP1B in this assay.

Dystonin Colocalizes with Clathrin Heavy Chain

Co-immunofluorescence experiments were conducted to validate the potential interaction between clathrin heavy chain and the plakin domain of dystonin-a. Cos-1 cells were transiently transfected with dyst-a2, and coimmunofluorescence analysis with endogenous clathrin heavy chain was conducted. Dyst-a2 was found to transfect approximately 11% of the cells observed (plating density of 40 000 cells per well in a 12-well plate). Figure 3A−C depicts colocalization of dyst-a2 with endogenous clathrin heavy chain in ~51% of dyst-a2 transfected cells. Overexpression of dyst-a2 in the transfected Cos-1 cells resulted in a change in the pattern of endogenous clathrin heavy chain localization (Figure 3C, inset). The clathrin heavy chain signal is altered from a diffuse punctate pattern throughout the cell to one localized specifically to the overexpression pattern of dyst-a2 (Figure 3A−C). This pattern of localization was observed in 38% of the transfected cells observed. The remaining transfected cells had very low endogenous clathrin heavy chain expression.

Clathrin Heavy Chain Association with Dystonin-a2 through Proximity Ligation Assay

As with MAP1B, clathrin heavy chain and dystonin were also shown to interact through PLA. Positive PLA signals were observed in Cos-1 cells that were transiently transfected with dyst-a2 and also expressing endogenous clathrin heavy chain (Figure 3D−F). Signals were not observed in cells that were not transfected with dyst-a2, but were expressing endogenous clathrin heavy chain, which is indicative of the specificity of the assay (Figure 3D, E).

Reciprocal Coimmunoprecipitation of Clathrin Heavy Chain and the Dystonin Plakin Domain

Co-immunoprecipitation experiments were performed using lysate from Cos-1 cells that were transiently transfected with Ntermlong or Daxx. Daxx was once again used as a negative control for the coimmunoprecipitation reactions. Ntermlong but not Daxx was reciprocally coimmunoprecipitated with endogenous clathrin heavy chain (Figure 3G). Additionally, immunoblots for flag and clathrin heavy chain were performed on the lysate from the transfected cells. Expression and binding of the flag epitopes to Dynal protein G beads was confirmed. Additionally, clathrin heavy chain was detected in both input lysates at ~170 kDa (Figure 3G).

In vivo Expression

Protein expression analysis for the identified interacting partners was conducted in the dt^{27J} mouse line. Protein levels of total MAP1B and clathrin heavy chain were unaltered in dt^{27J} DRGs at age P15, shortly after the onset of the phenotype (Figure 4). As

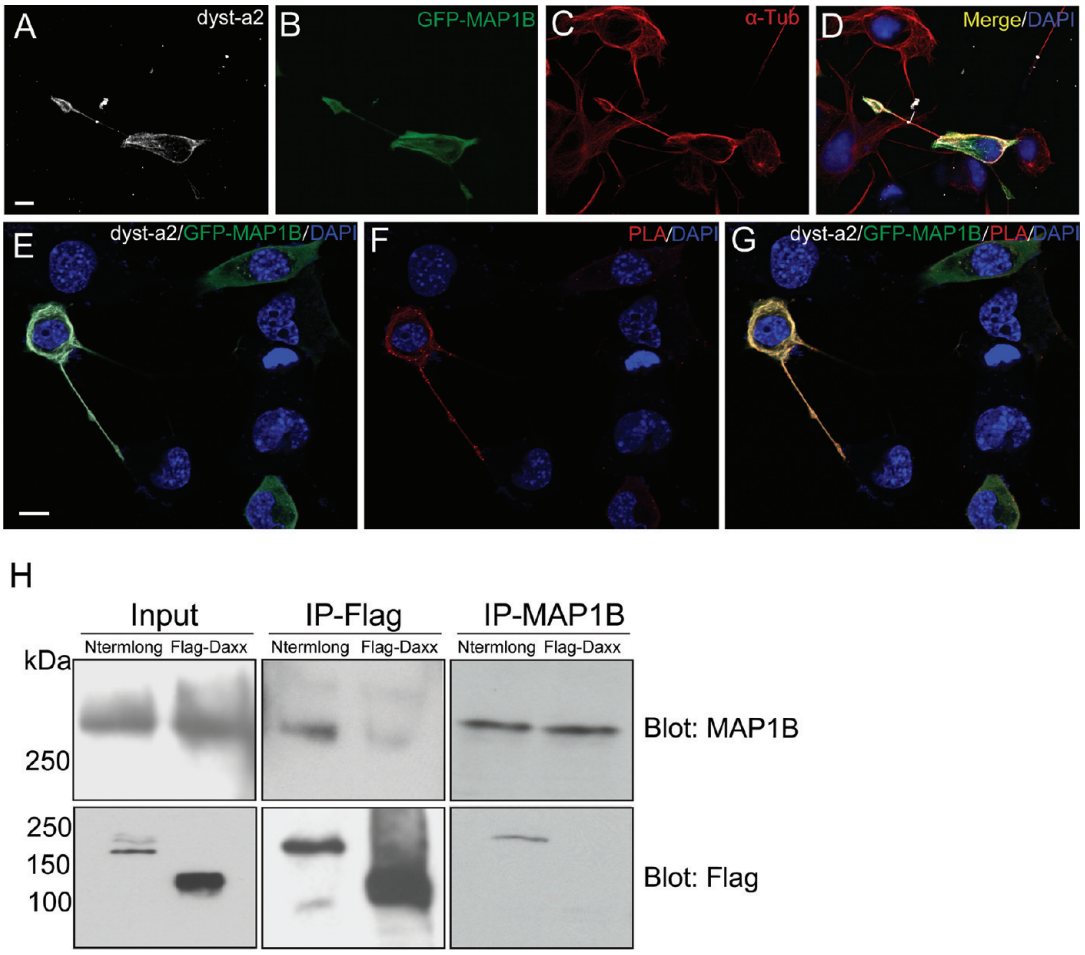

Figure 2. MAP1B and dystonin-a2 expression in F11 cells. (A–D) Full-length dystonin-a2 (dyst-a2) fusion plasmid encoding the structural components of the full-length dystonin-a2 with a myc-tag at the C-terminal end was transfected into F11 cells along with N-terminally tagged GFP-MAP1B. Cells were differentiated for 48 h. Confocal micrographs demonstrate the expression and colocalization of GFP-MAP1B (green) and dyst-a2 (white) in transfected F11 cells. The colocalization pattern of the two proteins occurred along the perinuclear region and extended throughout the cell body along with α-tubulin (α-tub) (red) in 38% of the transfected cells. Nuclei were stained with DAPI and are visualized in blue. Proximity ligation assay between dystonin and MAP1B in F11 cells. (E–G) Positive PLA signal (red) was observed in F11 cells cotransfected with both dyst-a2 (white) and GFP-MAP1B (green). Cells expressing only GFP-MAP1B did not express a positive PLA signal alluding to the specificity of the assay. (H) Reciprocal coimmunoprecipitation between Flag-tagged plakin domain (Ntermlong, ~170 kDa) and endogenous MAP1B in differentiated F11 cells supporting the potential of an interaction between these proteins. Flag-tagged death associated protein (Flag-Daxx, ~115 kDa) was used as a negative control for the immunoprecipitation reactions. Scale bar (10 μm) indicated in A is applicable to B–D as well. Scale bar (10 μm) indicated in E is applicable to F and G as well.

elevation in phosphorylated MAP1B is implicated in neurodegenerative disorders[29] we examined its levels in DRGs from *dt*^{27J} mice using SMI-31 antibody, which recognizes phosphoepitopes between amino acids 1244 and 1264 in the SPAKS sequence on MAP1B.[30] Phosphorylated MAP1B levels were significantly elevated ($p < 0.05$) in the *dt* DRGs when compared to wild type age matched controls in this tissue type (Figure 4).

DISCUSSION

The large multidomain structure of dystonin likely allows for it to participate in diverse cellular processes. Pull-down assays using the dystonin plakin domain to screen for interacting proteins within brain lysate has indicated several novel dystonin partners. Interactions between dystonin-a2 and MAP1B, and dystonin-a2 and clathrin heavy chain have been validated in this study using several techniques. A misregulation of phosphorylated MAP1B levels in *dt* mutant mice indicates a potential consequence of the loss of their interaction in these animals.

Dystonin Interaction with MAP1B

The interaction between MAP1B and the dystonin plakin domain may be explained by a potential interaction between a proline-rich region in the middle of MAP1B and the dystonin SH3 domain, though this remains to be demonstrated. MAP1B is a major cytoskeletal protein necessary for neurite outgrowth. It is the earliest MAP expressed in the embryonic brain, found abundantly in developing axons.[31,32] MAP1B is essential for neuritogenesis both in *in vivo* and *in vitro* model systems.[33] As it is one of the earliest MAPs observed in the developing nervous system, its role in differentiation, growth of neuronal processes and microtubule assembly is imperative to normal development.[34–37] Along with Tau and MAP2, MAP1B exhibits a synergistic role in neurite outgrowth. It is also essential for growth cone directionality and modulation of microtubule stability through its phosphorylation.[37–42]

The dystonin-MAP1B interaction may affect the regulation of MAP1B phosphorylation that occurs through proteins such as GSK3β.[30] The phosphorylation of MAP1B is an essential post-

dx.doi.org/10.1021/pr200564g |*J. Proteome Res.* 2011, 10, 5118–5127

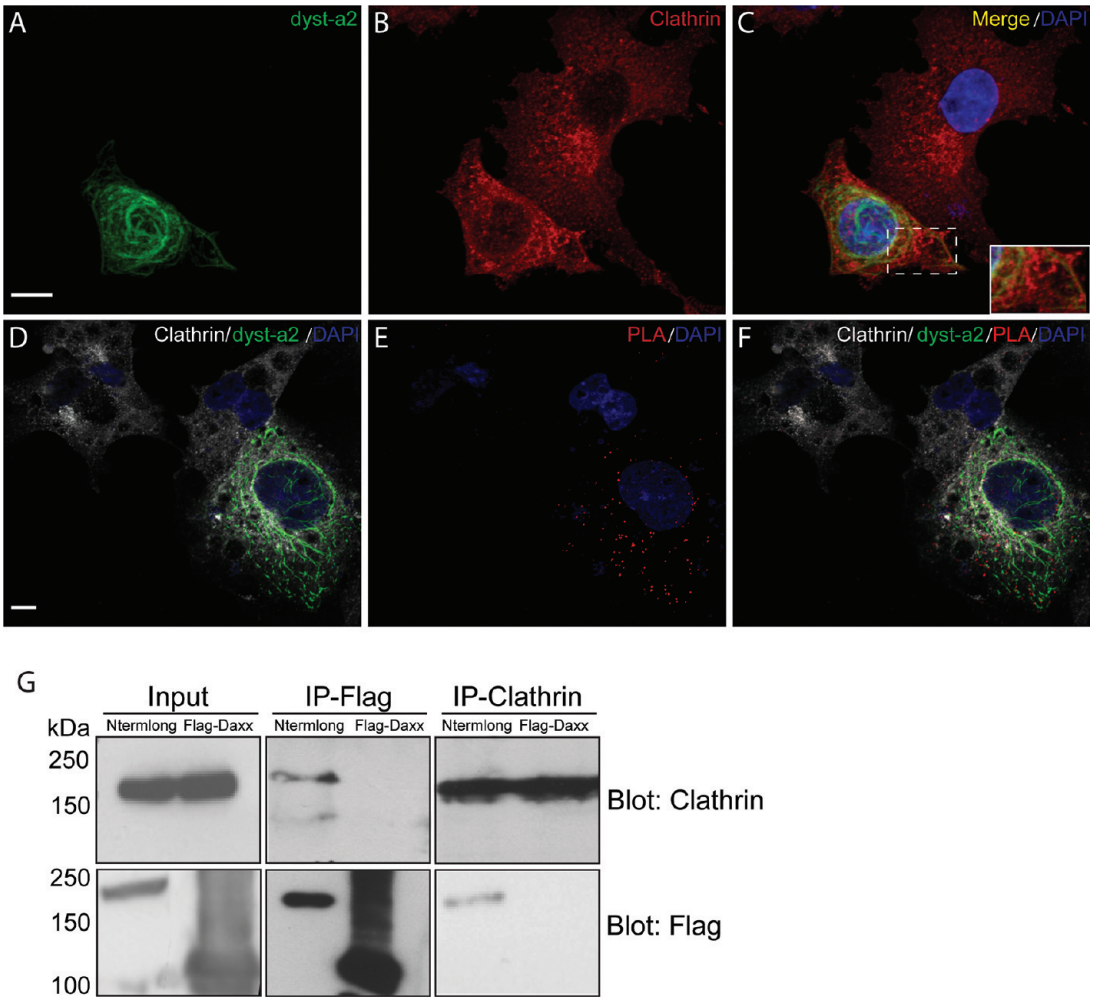

Figure 3. Clathrin heavy chain interacts with dystonin. Clathrin and dystonin-a2 expression in Cos-1 cells. (A−C) Full-length dystonin-a2 (dyst-a2) fusion plasmid encoding the structural components of the full-length dystonin-a2 with a myc-tag at the C-terminal end was transfected into Cos-1 cells. Confocal micrographs demonstrate the expression and colocalization of endogenous clathrin heavy chain (red) and dyst-a2 (green) in transfected Cos-1 cells. In nontransfected cells, endogenous clathrin expression was punctate and diffuse throughout the cell body with some polarized aggregation around the nucleus. However, in dyst-a2 transfected Cos-1 cells, the expression of clathrin was altered (C, inset). The reorganization of clathrin heavy chain signal colocalized with dyst-a2. The colocalization pattern occurred along the perinuclear region and extended throughout the cell body in 51% of the transfected cells. In the remaining transfected cells endogenous clathrin heavy chain signal was greatly reduced. Nuclei have been marked with DAPI nuclear stain and are visualized in blue. Proximity ligation assay between dystonin and clathrin heavy chain in F11 cells. (D−F) Positive PLA signal (red) was observed in Cos-1 cells transfected with dyst-a2 (green). Cells not transfected with dyst-a2, but expressing clathrin heavy chain (white) did not express a positive PLA signal, alluding to the specificity of the assay. (G) Reciprocal coimmunoprecipitation between Flag-tagged plakin domain (Ntermlong) and endogenous clathrin heavy chain in Cos-1 cells supporting the potential for an interaction between these proteins. Flag-tagged death associated protein (Flag-Daxx) was used a negative control for the immunoprecipitation reactions. Scale bar (10 μm) indicated in A is applicable to B and C as well. Scale bar (10 μm) indicated in D is applicable to E and F as well.

translational modification that modulates its function and contributes to its cellular activities. GSK3β phosphorylation events are part of a larger signaling cascade involving semaphorins, among several other upstream regulators.[43] As would be expected of such an integral protein, the aberrant functioning of MAP1B has been implicated in the manifestation of several neurodegenerative diseases. In addition to its role in tuberous sclerosis,[44,45] MAP1B (along with Tau) is proposed to contribute to early hippocampal neuropathy in Alzheimer's patients through its phosphorylation and potentially hyperphosphorylation.[29] As sensory neuropathy is a hallmark of the *dt* pathology, it is interesting that DRGs are the only tissue that express MAP1B at relatively high levels after MAP1B expression has significantly decreased in all other tissue.[46]

Dystonin-a Interaction with Clathrin—Implications for *dt* Pathology

An association with a trafficked noncytoskeletal cellular component such as clathrin, which is involved in endocytosis and synaptic vesicle recycling, once again raises the possibility of the involvement of a dystonin neuronal isoform in axonal trafficking. It is tempting to speculate how a neuronal dystonin isoform may be participating in this trafficking activity. Based on the role of clathrin in endocytosis and Golgi-exocytosis as well as synaptic vesicle recycling, and given the significant role of the actin cytoskeleton in mediating clathrin's activity, dystonin may play a role in associating these cellular components. As dorsal root sensory neurons possess comparatively lower levels of proteins such as MACF1 that can compensate for the loss of dystonin,[1] these neurons

dx.doi.org/10.1021/pr200564g |*J. Proteome Res.* 2011, 10, 5118–5127

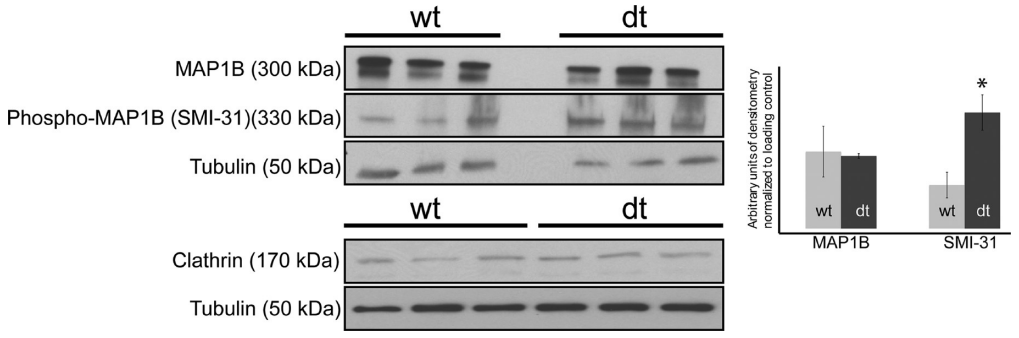

Figure 4. Western blot analysis of MAP1B, phosphorylated MAP1B and clathrin heavy chain protein levels in *dt* mice. MAP1B and phosphorylated MAP1B (detected using SMI31) levels were examined in DRG lysate from phenotype stage dt^{27J} and age-matched wild-type control mice. MAP1B protein level was unaltered in phenotype stage dt^{27J} mice. SMI31, which is used as a marker for phosphorylated MAP1B revealed a significantly elevated signal in phenotype stage dt^{27J} mice. Clathrin heavy chain was found to be unaltered in dt^{27J} mice when compared to wild-type age-matched controls. β-tubulin (tubulin) was used as a loading control. Asterisk indicates $p < 0.05$.

become the primary site for dysfunctions associated with the *dt* condition. Through a "dying back" phenomenon, the axonal defects could ultimately lead to neuronal death and present as the overt *dt* phenotype.

The existence of several neuronal dystonin isoforms suggests its involvement in numerous cellular activities. The association of dystonin-a2 with the endoplasmic reticulum, components of the nuclear envelope and the Golgi network supports the notion that disruption in dystonin functioning may result in protein processing anomalies contributing to the neuropathy of the *dt* condition.[11] An association with a coat protein such as clathrin may fit with such a hypothesis. As trans-Golgi transport is performed through the actions of clathrin and its associated proteins, a role for dystonin in trafficking along the axon can also be proposed. Loss of a dystonin neuronal isoform along the axon may disrupt axonal transport and further compound potential processing defects at the endoplasmic reticulum, ultimately leading to the *dt* phenotype.

CONCLUSION

The multidomain structure of dystonin makes it a likely candidate for interactions with various components of the cell. Previous characterization of this giant plakin protein has highlighted interactions with the major components of the cytoskeleton. The goal of the present study was to identify novel interacting partners of the plakin domain of neuronal dystonin. The initial pull-down screen identified several interesting candidates that warranted further analysis. Of the candidates identified, the cytoskeletal supporting protein MAP1B has helped further establish dystonin's potential role in modulating the cytoskeleton and link its various components. This interaction has also raised possible insight into the pathological progression of the *dt* condition through the modulation of phosphorylation events. Further investigation into dystonin's role in the functioning of MAP1B will advance our understanding of the biological relevance of this newly identified interaction and will help shed light on the *dt* condition. Interestingly, the interaction screen also revealed a novel noncytoskeletal dystonin interacting partner, clathrin heavy chain. In addition to facilitating our understanding of the diverse roles played by dystonin in the cell, this interaction raises numerous questions that suggest dystonin's involvement in both endocytosis and the late secretory pathway. Such an involvement brings to light a new, previously unknown role for dystonin that may help elucidate the etiology of the *dt* pathology, and better our understanding of cytoskeletal dynamics.

ASSOCIATED CONTENT

Supporting Information

This project was funded by a grant from the Canadian Institutes of Health Research (CIHR) to R.K. R.K. is a recipient of a University Health Research Chair from the University of Ottawa. This material is available free of charge via the Internet at http://pubs.acs.org.

AUTHOR INFORMATION

Corresponding Author

*Tel: 613-737-8707. Fax: 613-737-8803. E-mail: rkothary@ohri.ca.

Present Addresses

‡Institute for Biological Sciences, National Research Council Canada, Bldg. M-54, 1200 Montreal Rd., Ottawa, Canada, K1A 0R6

ACKNOWLEDGMENT

We are grateful to Mr. Justin G. Boyer for critical reading of the manuscript and the rest of the Kothary laboratory for helpful discussions. We also thank Dr. David Picketts (OHRI, Ottawa) for the Flag-Daxx plasmid, Dr. Gordon-Weeks (King's College, London) for the GFP-MAP1B plasmid, and Drs. Shaun Beug and Valerie Wallace (OHRI, Ottawa) for the rat brain lysate.

REFERENCES

(1) Ruhrberg, C.; Watt, F. M. The plakin family: versatile organizers of cytoskeletal architecture. *Curr. Opin. Genet. Dev.* **1997**, *7* (3), 392–7.

(2) (a) Röper, K.; Gregory, S. L.; Brown, N. H. The 'spectraplakins': cytoskeletal giants with characteristics of both spectrin and plakin families. *J. CellSci.* **2002**, *115* (Pt 22), 4215–25. (b) Sonnenberg, A.; Liem, R. K. Plakins in development and disease. *Exp. Cell Res.* **2007**, *313* (10), 2189–203. (c) Boyer, J. G.; Bernstein, M. A.; Boudreau-Lariviere, C. Plakins in striated muscle. *Muscle Nerve* **2010**, *41* (3), 299–308.

(3) Young, K. G.; Kothary, R. Dystonin/Bpag1--a link to what? *Cell Motil Cytoskeleton* **2007**, *64* (12), 897–905.

(4) Duchen, L. W.; Falconer, D. S.; Strich, S. J. Dystonia Musculorum. A hereditary neuropathy of mice affecting mainly sensory pathways. *J. Physiol.* **1963**, *165*, 7–9.
(5) Brown, A.; Bernier, G.; Mathieu, M.; Rossant, J.; Kothary, R. The mouse dystonia musculorum gene is a neural isoform of bullous pemphigoid antigen 1. *Nat. Genet.* **1995**, *10* (3), 301–6.
(6) Guo, L.; Degenstein, L.; Dowling, J.; Yu, Q. C.; Wollmann, R.; Perman, B.; Fuchs, E. Gene targeting of BPAG1: abnormalities in mechanical strength and cell migration in stratified epithelia and neurologic degeneration. *Cell* **1995**, *81* (2), 233–43.
(7) Duchen, L. W.; Strich, S. J. Clinical and pathological studies of an hereditary neuropathy in mice. *Brain* **1964**, *87*, 367–378.
(8) al-Ali, S. Y.; al-Zuhair, A. G. Fine structural study of the spinal cord and spinal ganglia in mice afflicted with a hereditary sensory neuropathy, dystonia musculorum. *J. Submicrosc. Cytol. Pathol.* **1989**, *21* (4), 737–48.
(9) Bernier, G.; Kothary, R. Prenatal onset of axonopathy in Dystonia musculorum mice. *Dev. Genet.* **1998**, *22* (2), 160–8.
(10) Sotelo, C.; Guenet, J. L. Pathologic changes in the CNS of dystonia musculorum mutant mouse: an animal model for human spinocerebellar ataxia. *Neuroscience* **1988**, *27* (2), 403–24.
(11) Young, K. G.; Kothary, R. Dystonin/Bpag1 is a necessary endoplasmic reticulum/nuclear envelope protein in sensory neurons. *Exp. Cell Res.* **2008**, *314* (15), 2750–61.
(12) De Repentigny, Y.; Ferrier, A.; Ryan, S. D.; Sato, T.; Kothary, R. Motor unit abnormalities in dystonia musculorum mice. *PLoS One* **2011**, *6* (6), e21093.
(13) Brown, A.; Dalpe, G.; Mathieu, M.; Kothary, R. Cloning and characterization of the neural isoforms of human dystonin. *Genomics* **1995**, *29* (3), 777–80.
(14) Leung, C. L.; Zheng, M.; Prater, S. M.; Liem, R. K. The BPAG1 locus: alternative splicing produces multiple isoforms with distinct cytoskeletal linker domains, including predominant isoforms in neurons and muscles. *J. Cell Biol.* **2001**, *154* (4), 691–8.
(15) Young, K. G.; Pinheiro, B.; Kothary, R. A Bpag1 isoform involved in cytoskeletal organization surrounding the nucleus. *Exp. Cell Res.* **2006**, *312* (2), 121–34.
(16) Jefferson, J. J.; Leung, C. L.; Liem, R. K. Dissecting the sequence specific functions of alternative N-terminal isoforms of mouse bullous pemphigoid antigen 1. *Exp. Cell Res.* **2006**, *312* (15), 2712–25.
(17) Young, K. G.; Pool, M.; Kothary, R. Bpag1 localization to actin filaments and to the nucleus is regulated by its N-terminus. *J. Cell Sci.* **2003**, *116* (Pt 22), 4543–55.
(18) Sun, D.; Leung, C. L.; Liem, R. K. Characterization of the microtubule binding domain of microtubule actin crosslinking factor (MACF): identification of a novel group of microtubule associated proteins. *J. Cell Sci.* **2001**, *114* (Pt 1), 161–172.
(19) Boyer, J. G.; Bhanot, K.; Kothary, R.; Boudreau-Lariviere, C. Hearts of dystonia musculorum mice display normal morphological and histological features but show signs of cardiac stress. *PLoS One* **2010**, *5* (3), e9465.
(20) Koster, J.; Geerts, D.; Favre, B.; Borradori, L.; Sonnenberg, A. Analysis of the interactions between BP180, BP230, plectin and the integrin alpha6beta4 important for hemidesmosome assembly. *J. Cell Sci.* **2003**, *116* (Pt 2), 387–99.
(21) (a) Favre, B.; Fontao, L.; Koster, J.; Shafaatian, R.; Jaunin, F.; Saurat, J. H.; Sonnenberg, A.; Borradori, L. The hemidesmosomal protein bullous pemphigoid antigen 1 and the integrin beta 4 subunit bind to ERBIN. Molecular cloning of multiple alternative splice variants of ERBIN and analysis of their tissue expression. *J. Biol. Chem.* **2001**, *276* (35), 32427–36. (b) Jefferson, J. J.; Ciatto, C.; Shapiro, L.; Liem, R. K. Structural analysis of the plakin domain of bullous pemphigoid antigen1 (BPAG1) suggests that plakins are members of the spectrin superfamily. *J. Mol. Biol.* **2007**, *366* (1), 244–57.
(22) Hansson, H.; Okoh, M. P.; Smith, C. I.; Vihinen, M.; Hard, T. Intermolecular interactions between the SH3 domain and the proline-rich TH region of Bruton's tyrosine kinase. *FEBS Lett.* **2001**, *489* (1), 67–70.
(23) Kay, B. K.; Williamson, M. P.; Sudol, M. The importance of being proline: the interaction of proline-rich motifs in signaling proteins with their cognate domains. *FASEB J.* **2000**, *14* (2), 231–41.
(24) Yu, H.; Chen, J. K.; Feng, S.; Dalgarno, D. C.; Brauer, A. W.; Schreiber, S. L. Structural basis for the binding of proline-rich peptides to SH3 domains. *Cell* **1994**, *76* (5), 933–45.
(25) Woods, C. M.; Lazarides, E. Spectrin assembly in avian erythroid development is determined by competing reactions of subunit homo- and hetero-oligomerization. *Nature* **1986**, *321* (6065), 85–9.
(26) Wilm, M.; Shevchenko, A.; Houthaeve, T.; Breit, S.; Schweigerer, L.; Fotsis, T.; Mann, M. Femtomole sequencing of proteins from polyacrylamide gels by nano-electrospray mass spectrometry. *Nature* **1996**, *379* (6564), 466–9.
(27) Shafey, D.; Boyer, J. G.; Bhanot, K.; Kothary, R. Identification of novel interacting protein partners of SMN using tandem affinity purification. *J. Proteome Res.* **2010**, *9* (4), 1659–69.
(28) Elias, J. E.; Haas, W.; Faherty, B. K.; Gygi, S. P. Comparative evaluation of mass spectrometry platforms used in large-scale proteomics investigations. *Nat. Methods* **2005**, *2* (9), 667–75.
(29) Good, P. F.; Alapat, D.; Hsu, A.; Chu, C.; Perl, D.; Wen, X.; Burstein, D. E.; Kohtz, D. S. A role for semaphorin 3A signaling in the degeneration of hippocampal neurons during Alzheimer's disease. *J. Neurochem.* **2004**, *91* (3), 716–36.
(30) Trivedi, N.; Marsh, P.; Goold, R. G.; Wood-Kaczmar, A.; Gordon-Weeks, P. R. Glycogen synthase kinase-3beta phosphorylation of MAP1B at Ser1260 and Thr1265 is spatially restricted to growing axons. *J. Cell Sci.* **2005**, *118* (Pt 5), 993–1005.
(31) Matus, A.; Riederer, B. Microtubule-associated proteins in the developing brain. *Ann. N.Y. Acad. Sci.* **1986**, *466*, 167–79.
(32) Tucker, R. P.; Garner, C. C.; Matus, A. In situ localization of microtubule-associated protein mRNA in the developing and adult rat brain. *Neuron* **1989**, *2* (3), 1245–56.
(33) Gonzalez-Billault, C.; Owen, R.; Gordon-Weeks, P. R.; Avila, J. Microtubule-associated protein 1B is involved in the initial stages of axonogenesis in peripheral nervous system cultured neurons. *Brain Res.* **2002**, *943* (1), 56–67.
(34) Pedrotti, B.; Islam, K. Microtubule associated protein 1B (MAP1B) promotes efficient tubulin polymerisation in vitro. *FEBS Lett.* **1995**, *371* (1), 29–31.
(35) Riederer, B.; Cohen, R.; Matus, A. MAP5: a novel brain microtubule-associated protein under strong developmental regulation. *J. Neurocytol.* **1986**, *15* (6), 763–75.
(36) Tucker, R. P.; Binder, L. I.; Matus, A. I. Neuronal microtubule-associated proteins in the embryonic avian spinal cord. *J. Comp. Neurol.* **1988**, *271* (1), 44–55.
(37) Brugg, B.; Matus, A. PC12 cells express juvenile microtubule-associated proteins during nerve growth factor-induced neurite outgrowth. *J. Cell Biol.* **1988**, *107* (2), 643–50.
(38) Gonzalez-Billault, C.; Engelke, M.; Jimenez-Mateos, E. M.; Wandosell, F.; Caceres, A.; Avila, J. Participation of structural microtubule-associated proteins (MAPs) in the development of neuronal polarity. *J. Neurosci. Res.* **2002**, *67* (6), 713–9.
(39) Garcia, M. L.; Cleveland, D. W. Going new places using an old MAP: tau, microtubules and human neurodegenerative disease. *Curr. Opin. Cell Biol.* **2001**, *13* (1), 41–8.
(40) Takei, Y.; Teng, J.; Harada, A.; Hirokawa, N. Defects in axonal elongation and neuronal migration in mice with disrupted tau and map1b genes. *J. Cell Biol.* **2000**, *150* (5), 989–1000.
(41) Mack, T. G.; Koester, M. P.; Pollerberg, G. E. The microtubule-associated protein MAP1B is involved in local stabilization of turning growth cones. *Mol. Cell. Neurosci.* **2000**, *15* (1), 51–65.
(42) Mansfield, S. G.; Diaz-Nido, J.; Gordon-Weeks, P. R.; Avila, J. The distribution and phosphorylation of the microtubule-associated protein MAP 1B in growth cones. *J. Neurocytol.* **1991**, *20* (12), 1007–22.
(43) Zhou, F. Q.; Snider, W. D. CELL BIOLOGY: GSK-3beta and Microtubule Assembly in Axons. *Science* **2005**, *308* (5719), 211–4.
(44) Ding, J.; Liu, J. J.; Kowal, A. S.; Nardine, T.; Bhattacharya, P.; Lee, A.; Yang, Y. Microtubule-associated protein 1B: a neuronal binding partner for gigaxonin. *J. Cell Biol.* **2002**, *158* (3), 427–33.

(45) Yamanouchi, H.; Jay, V.; Rutka, J. T.; Takashima, S.; Becker, L. E. Evidence of abnormal differentiation in giant cells of tuberous sclerosis. *Pediatr. Neurol.* **1997**, *17* (1), 49–53.

(46) Ma, D.; Nothias, F.; Boyne, L. J.; Fischer, I. Differential regulation of microtubule-associated protein 1B (MAP1B) in rat CNS and PNS during development. *J. Neurosci. Res.* **1997**, *49* (3), 319–32.